LUND UNIVERSITY

Multicolor fluorescence imaging-system for tissue diagnostics

Andersson-Engels, Stefan; Johansson, Jonas; Svanberg, Sune

Link to publication

Multicolor fluorescence imaging system for tissue diagnostics

Stefan Andersson-Engels, Jonas Johansson and Sune Svanberg

Department of Physics, Lund Institute of Technology,
P.O. Box 118, S-221 00 Lund, Sweden

ABSTRACT

A multicolor fluorescence imaging system for tissue diagnostics has been constructed. Examples given to illustrate the system performance are atherosclerotic plaque lesions from human artery samples and a malignant rat brain tumor model. The system simultaneously monitors fluorescence images at four different wavelengths, enabling spatial as well as spectral information to be extracted. By selection of band pass filters an artificial image of the lesion under study can be formed, based on an optimal contrast function of four fluorescence intensities. The image is constructed in a computer and displayed in false colors on a monitor. Pulsed excitation light from an N2 laser provides the possibility of using a gated detector, and in this way suppress room light to an undetectable level. Images can thus be recorded under white light illumination during visual inspection, increasing the usefulness of the system.

1. INTRODUCTION

Diagnostic techniques for localizing diseased tissue are of great medical interest. Complementary to other existing techniques, laser-induced fluorescence for tissue diagnostics is being developed. Animal experiments as well as clinical studies have been performed to investigate tissue fluorescence characteristics and to evaluate their usefulness. The main fields of interest have been the identification of malignant tumors and atherosclerotic plaques. The intrinsic tissue autofluorescence has been utilized [1-6] as well as enhanced fluorescence utilizing fluorescent tumor marking drugs [7-11]. The tumor marking drug hematoporphyrin derivative (HpD) has been used almost exclusively. The development of other drugs is in progress [12].

Generally, only the fluorescence intensity in one particalar wavelength band has been used in diagnostics. To improve diagnostics techniques several fluorescence intensities should be recorded. Two principally different methods can be used, measuring the total fluorescence intensity as a function of excitation wavelength (excitation spectra) or monitoring the distribution of emission wavelengths for a fixed excitation wavelength (emission spectra). The total time-integrated emission can be measured, or the intensity as a function of delay time after pulsed excitation can be monitored. The simplest and most frequently used method is the measurement of fluorescence emission spectra. Simple signal processing routines have been proposed to improve tissue diagnostic criteria. Profio *et al.* measured the fluorescence intensity in two fluorescence bands in order to subtract the tissue autofluorescence from the fluorescence resulting from the tumor marking drug [13]. By forming a ratio of two intensities insensitivity to instrumental parameters, such as detection geometry and source fluctuations is obtained [14,15]. These evaluation procedures have led to improved tissue demarcation, increased stability and better correlation with other diagnostic techniques.

Imaging techniques are required in order to visualize the diseased region. Various systems have been developed for this purpose [16-18]. One of these systems records the fluorescence intensity at one wavelength and displays it [16], in another the tissue autofluorescence background is subracted by monitoring two different fluorescence bands [17] and in a third system the autofluorescence background is subtracted by employing a differential excitation technique [18]. Simultaneous recording of the images in the different fluorescence bands utilized in the evaluation is important if the object is moving or changing in some respect, preventing sequential recordings of the various fluorescence bands. Such techniques for medical use were tested by us using a linear diode array detector [19,20].

This paper describes a new system based on a nitrogen laser, a specially developed telescope, and a detector with a gatable image intensifier and a CCD camera. This instrumentation simultaneously records four images in selected fluorescence bands of the imaged tissue, and forms a mathematical function of these fluorescence intensities to present a false-colored artificial image of the object. The various colors indicate the fluorescence function value. This is high for a diseased region and low for normal unaffected tissue.

2. INSTRUMENTATION

A diagram of the experimental arrangement is shown in Fig. 1. As an excitation source a pulsed nitrogen (N2) laser is used (PRA LN250). The laser provides UV light with a wavelength of 337 nm in 3 ns long pulses. The laser is equipped with an electric filter on the power supply to reduce electromagnetic interference from the discharge in the laser tube and avoid detector noise. The laser beam is shaped with cylindrical quartz lenses to irradiate a quadratic area of variable size, typically 10 times 10 mm. The laser light is reflected from a dichroic mirror to irradiate the sample. The fluorescent light is collected in the backward direction with a specially designed Cassegrainian telescope. The specially designed telescope has a primary mirror split into four parts, each somewhat tilted off the optical axis. This arrangement allows each mirror segment to produce an image of the object a small distance off the optical axis in the image plane. It is thus possible to place the four identical images of the object on the four quadrants of an imaging detector. To extract the spectral information from the fluorescence signal, the fluorescence light collected by each mirror segment is filtered through the bandpass filter defining the fluorescence band of the image formed by this segment. In this way the object forms four images in different fluorescence bands on the four detector quadrants, using the same laser excitation pulse. The detector is a Delli Delti image-intensified CCD camera system, Model CPI/NS2 (modified). The image intensifier, which is lens coupled to the CCD camera, is a dual-stage micro-channel plate with an S20R photocathode response, gatable down to 5 ns. The pulsed excitation and gated detection allows CW background light to be suppressed to an undetectable level. The synchronization between the camera and the laser excitation is taken from the frame synchronization signal in the camera. This synchronization signal generates a common trigger signal which is fed to the laser and the image intensifier. The trigger signal to the laser passes an opto-coupler to prevent pick-up of noise from the laser discharge in the electronic supply to the image intensifier, with multi-triggering of the image intensifier as a result. An internal delay unit in the electric supply to the image intensifier enables exact synchronization between the laser and the image intensifier.
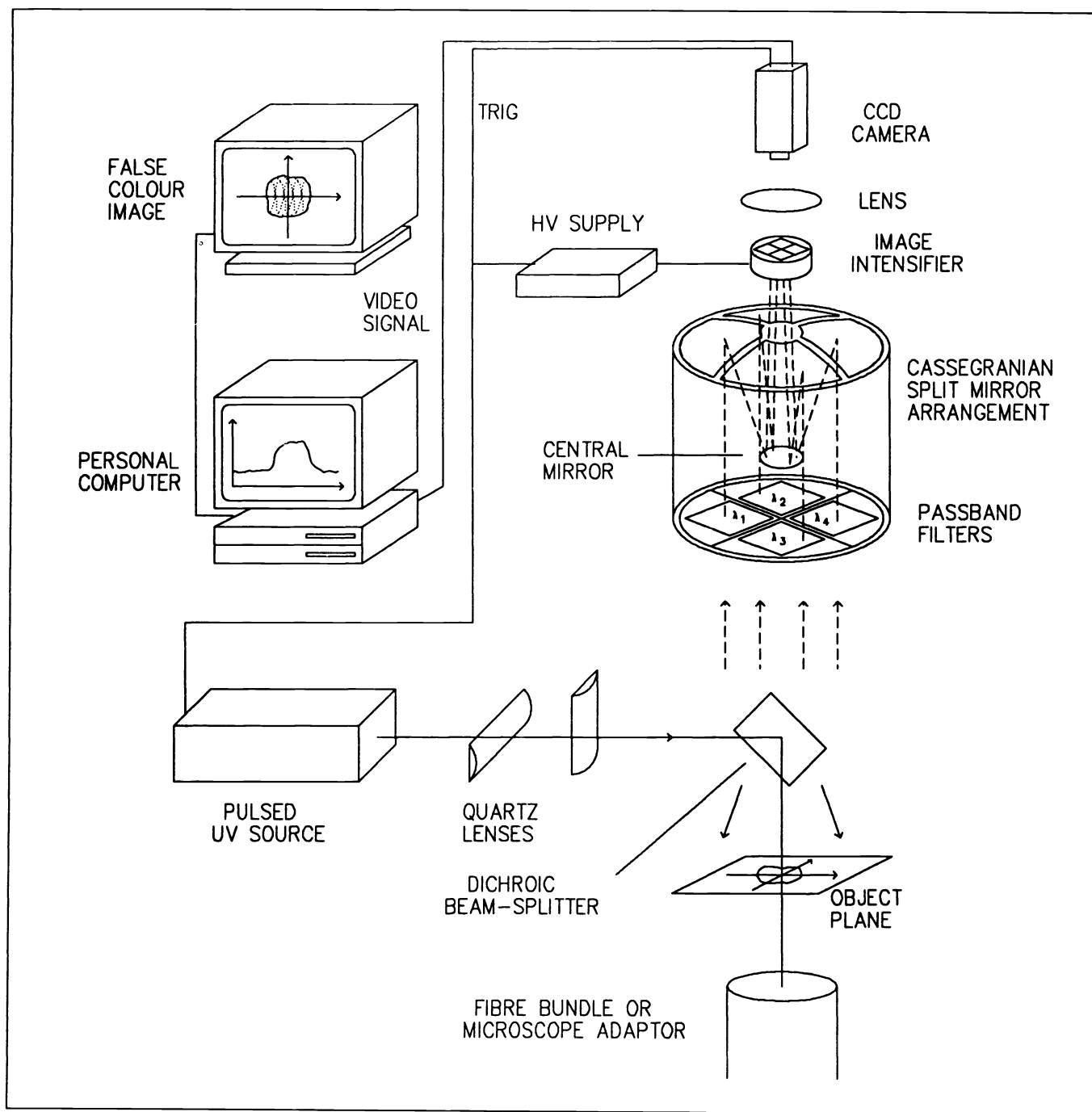
Fig. 1. Schematic arrangement of the fluorescence imaging system.

The standard CCIR video signal from the CCD camera is fed to a frame grabber (Data Translation DT2851) in a 386/387 IBM compatible personal computer. The formation of the artificial contrast-enhancing image from the four spectrally filtered images includes non-standard operations, which are not included in standard image analysis software. To speed up these calculations an extra array processor (Data Translation DT7020) is coupled directly to the frame grabber, without using the PC bus. Software for image recording and analysis is being developed.

The setup is run at a fixed focal length and image size. Altering these settings requires an optical adjustment of the four mirror segments, since they image the object off the optical axis. Before recording a fluorescence image, it is best to record the detector dark current. An image of this is stored in the computer. In order to obtain high quality images the response of the entire system should be measured and corrected for. Once this apparatus function is known it is not necessary for the system to have exactly the same response over the entire detector area. The system sensitivity can be measured by imaging an object which fluoresces in all detection bands with known relative intensities. The object must be structureless over the whole measured area. A fluorescence image of this object is also recorded and stored in the computer. After recording the images from the sample under study, the detector dark current image is subtracted, and the resulting image is divided by the detector response image. The function used to produce the artificial contrast-enhancing image from the four subimages is then applied. The results are presented on a video monitor.

3. SAMPLES

Two different kinds of tissue were examined, human atherosclerotic plaque and a rat brain tumor model. The human artery samples with atherosclerotic plaque lesions obtained from autopsies were examined within 2 days *post mortem* and within 2 hours after excision. The samples were rinsed clean from blood. The fluorescence was studied under the same conditions as those described in Ref. [21] with the samples irradiated in air.

The brain tumor was obtained from the right hemisphere of a Fischer-344 rat after inoculation of RG-2 cells. This cell line originates from ethyl nitrosurea-induced glioma in rats. The tumor grew to a size of 6 mm in diameter at the brain surface. Twenty-four hours before the animal was sacrificed and fluorescence imaging was performed, 5 mg/kg body weight Photofrin II (Quadra Logic Technologies, Vancouver) was injected intravenously into the animal. For the investigation the rat was sacrificed and the brain removed from the skull. The studies were carried out as described in Ref. [22] within 2 hours *post mortem* with the brain in an air environment.

4. SYSTEM PERFORMANCE

The smallest detectable signal is limited by the dark current in the MCPs and the CCD camera. The dynamic range of the detector will therefore be dependent on the level of the dark current in the detector. This was measured to be about 5 % of the saturation signal for a single stage MCP limited by the CCD camera and up to 10 % with the dual intensifier. The higher value of the dark current in the dual intensifier is due to its high internal gain amplifying the dark current from the first photocathode. In order to check the linearity of the detector response, a number of different neutral density filters were inserted in the filter holder. The results for a singel stage microchannel plate can be seen in Fig. 2. The linearity of the camera was found to be good in the light level interval of interest.
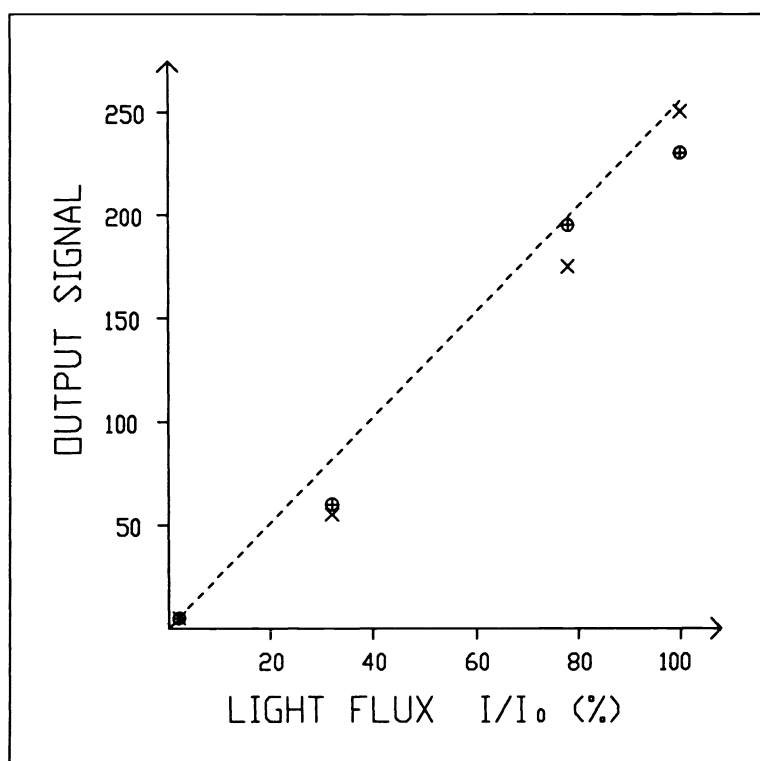
Fig. 2. Plot of the detector output signal (0-255) as a function of the light flux.

Four fluorescence images of a heavy fuel oil, seen through 3 mm thick Schott 420 nm cut-off filters used to suppress scattered laser light, were used to obtain the system response in the various pixels. Oil was chosen because of its broad fluorescence spectrum, homogeneous surface and small penetration depth for light. These parameters are important to ensure as smooth fluorescence characteristics as possible of an object in a well defined object plane. Light scattering in the sample must be negligible. Since all subimages display the same object and are filtered through the same filters, they should be identical. Any differences are due to imperfections in the detector. A honeycomb pattern originates from the pattern of the fiber bundles in the fiber-optic faceplate in the image intensifier. Also, the CCD camera elements have slightly different sensitivities, probably due to a spread in the active area of the various elements. One can also see that the object is not exposed to the same amount of excitation energy in all regions, but the images are brighter in some regions than in others.

All these effects are present for all images, and they can thus be corrected for by dividing all the images obtained by this system sensitivity image. An example of this is shown in Fig. 3a and b. Fig. 3a shows a test image used to investigate the spatial resolution of the system. Vertical lines with different spatial resolutions are imaged. Fig. 3b shows the same image but this time corrected for the system sensitivity. The outer regions appear to be much brighter in the corrected image, showing that these regions were not exposed as much as the central regions. Also, more even intensity can be seen in the white regions, due to corrections for the camera element sensitivity. The dark region caused by a burned spot in the MCP cannot be totally compensated for, since the transmission in this region is too low. Fig. 3c show the corresponding scans through the images. As can be seen, the spatial resolution of the system is of the order of 80 lines across an image, probably limited by the MCP.
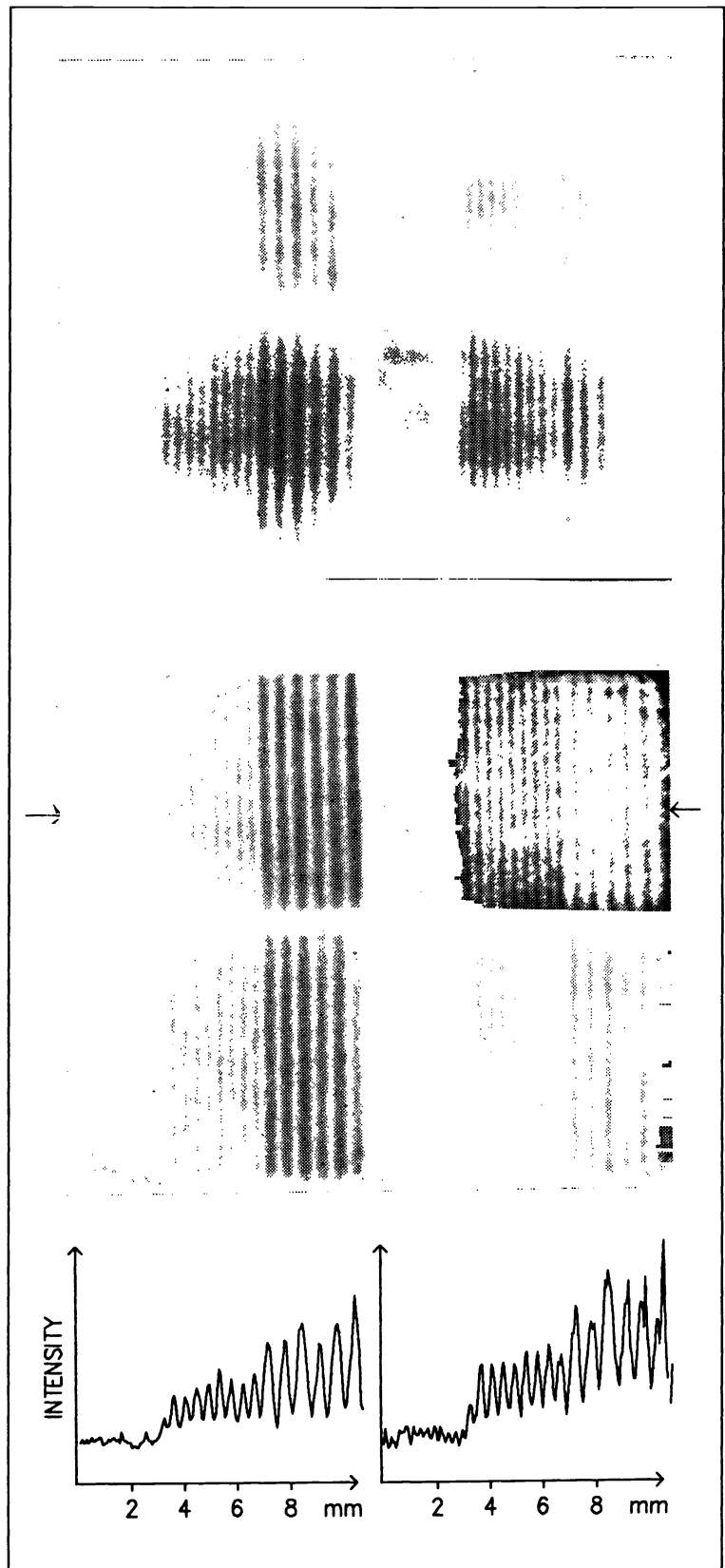
Fig. 3. *(a)* Direct fluorescence recording of striped paper as a test object. Detection filters were Schott GG 420 nm and the excitation source was filtered through a neutral density filter to reduce the intensity. *(b)* The same image as *(a)* but corrected with the system correction image obtained from a recording on a heavy oil sample. *(c)* A line scan through *(b)* as indicated in the figure.

a

FLUORESCENCE INTENSITY (rel. units)

ATHEROSCLEROTIC PLAQUE

NORMAL AORTA

400   500   600

WAVELENGTH/nm

b

500 nm   600 nm

450 nm   390 nm

c

INTENSITY

2 4 6 8 mm   2 4 6 8 mm

INTENSITY

2 4 6 8 mm   2 4 6 8 mm
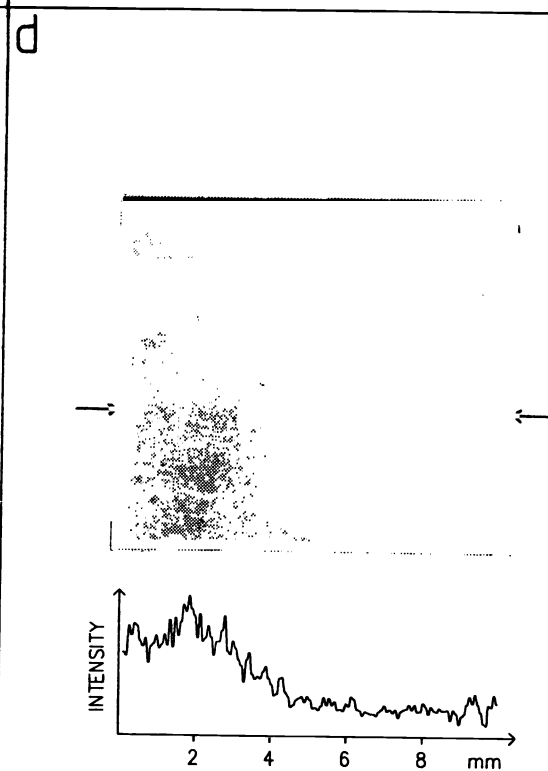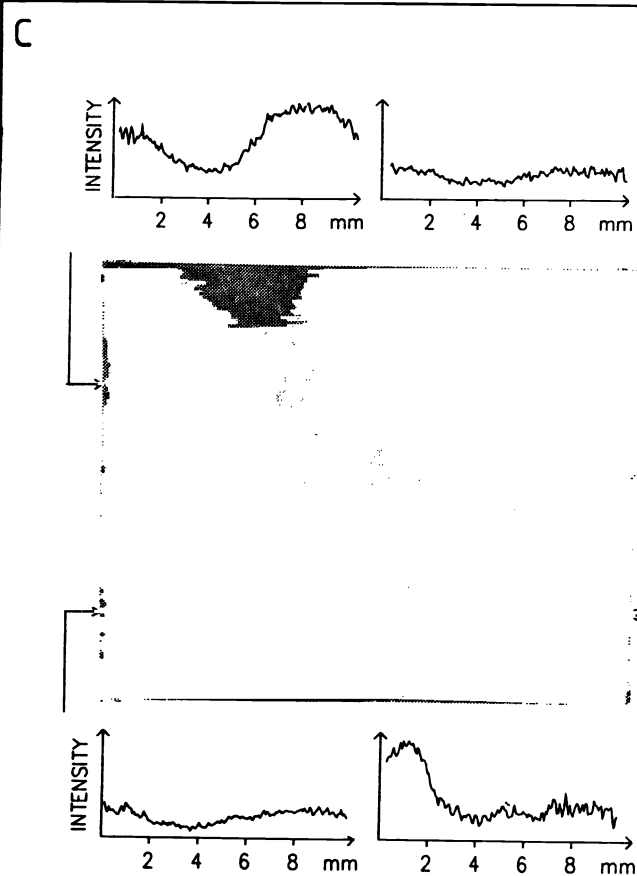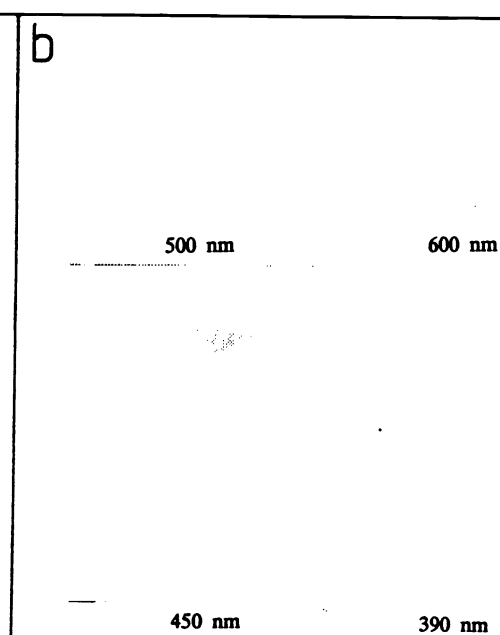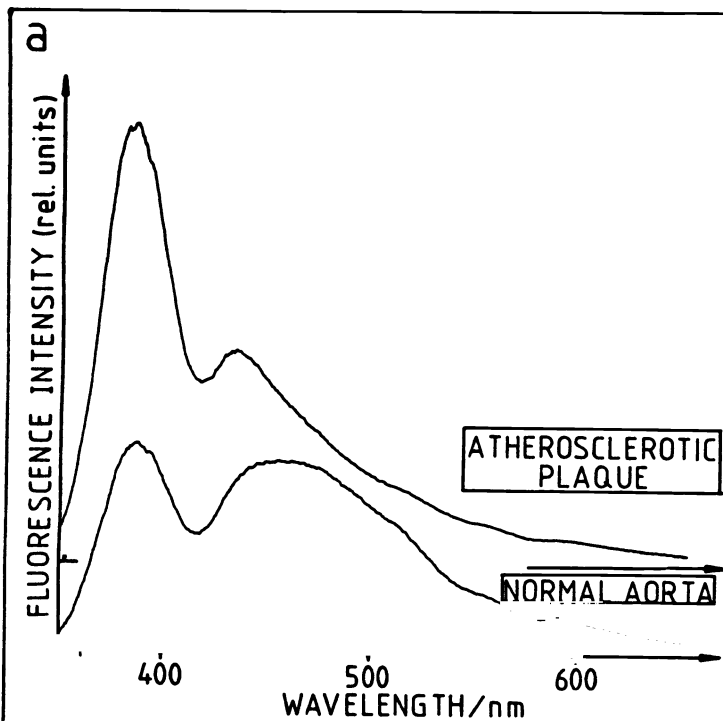
d

INTENSITY

2   4   6   8   mm

Fig. 4. *(a)* Fluorescence spectra of a normal aortic wall and a region of atherosclerotic plaque. Excitation wavelength 337 nm. *(b)* Total raw CCD camera image of an aortic sample with an atherosclerotic plaque region in the lower left corner. *(c)* The same image as in *(b)*, but corrected for the system response. Scans across the images in indicated positions are given. *(d)* Dimensionless artificial image constructed from *(c)* The function (I(390 nm)/I(450 nm)) demarcates the atherosclerotic plaque region. A line scan through the figure in indicated position is given.

Fluorescence spectra for normal artery wall and an atherosclerotic plaque region are shown in Fig. 4a, indicating four characteristic wavelength regions selected for imaging. In Fig. 4b the four fluorescence subimages of an artery sample are shown, filtered through different bandpass filters. An atherosclerotic plaque region in the lower left corner can be seen as a bright region at 390 nm and a darker region at 450 and 470 nm. The ratio between the 390 nm and the 450 nm subimages should yield a high value for the plaque region and a low value for the surrounding normal vessel wall. This is shown in Fig. 4c.

Fluorescence spectra of the rat brain tumor and the normal surrounding brain are shown in Fig. 5a. Wavelength bands selected for fluorescence imaging are indicated as in Ref. 21 as A' (630 nm), B (470 nm), C (690 nm) and D (600 nm). The dimensionless function (A'-D)/B is chosen as the tumor marking function. An artificial image is obtained from the system with this function as shown in Fig. 5b. The tumor region is situated in the lower right corner as seen in the figure.

DISCUSSION

In its present configuration, the system is suitable for laboratory studies. It can, however, with some development be used clinically. The optics will then be adjusted to image the exit surface of a fiberoptic imaging bundle. This surface then always defines the object plane for the telescope. Since the system works best with a fixed focal length, the arrangement with an optical fiber bundle matches the detection system well.

This system constitutes an improvement over existing medical imaging fluorosensors in several ways, but it also has certain drawbacks. The formation of a dimensionless quantity makes the system insensitive to light collection geometry and detection efficiency as well as to the excitation light distribution over the imaged area. The simultaneous detection of the four images enables the recording of correct images even during tissue or fiber-optical movements. Spatial as well as energy fluctuations for sequential pulses from the excitation source also cancel. The pulsed excitation and gated detection technique also allows the use of continuous white light, enabling visual inspection during recordings. The fact that the detector is divided into four parts, each imaging the object at one fluorescence wavelength, limits the resolution. However, when studying tissue fluorescence, at least in the red wavelength region, the resolution is usually set by the light scattering in tissue. In the red wavelength region light penetrates tissue relatively deeply. Small imperfections in the micro-channel plate (MCP) or CCD camera are compensated for with this system by correcting each image with a recorded system sensitivity image. This problem can also be compensated for by measuring the four images sequentially, and then forming the dimensionless function. For such a system no system sensitivity image would be necessary, thus saving time in the production of the image. Heavily burned-in spots
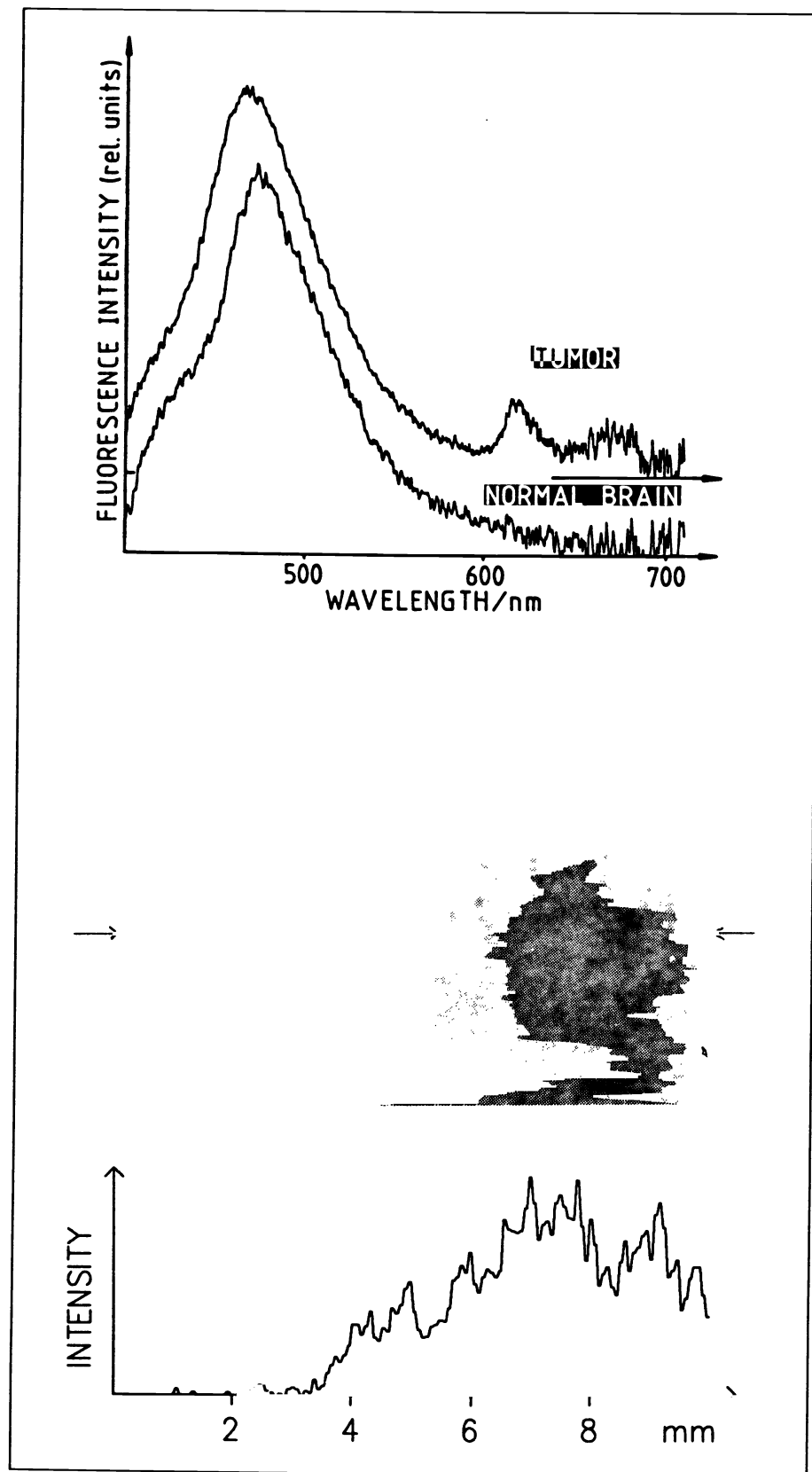
Fig.5. *(a)* Fluorescence spectra of a rat brain and a brain tumor, from a rat injected with Photofrin II 24 hours before the investigation. *(b)* Calculated artificial image using the dimensionless function (A'-D)/B

in the MCP with no transmission cannot be compensated for in either system. Another advantage with this system is that no moving parts are necessary, as in sequential recordings of the object in different fluorescence bands. The main limitation with this system is the time required for the image formation in the computer. The image formation from the subimages takes a few seconds in this system. While real-time display of the object in four bands is obtained, fully processed images are updated every few seconds. If the system corrections are small, near real-time processing of uncorrected, contrast-enhanced images can be obtained.

This instrumentation can have a wide field of applications outside medical diagnostics, e.g. in combustion, environmental and forensic research.

REFERENCES

1. Yuanlong Yang, Yanming Ye, Fuming Li, Yufen Li, Paozhong M, *Characteristic auto-fluorescence for cancer diagnosis and its origin*. Lasers Surg Med 1987, **7**:528-32
2. Alfano RR, Darayash BT, Cordero J, Tomashefsky P, Longo FW, Alfano MA, *Laser induced fluorescence spectroscopy from native cancerous and normal tissue*. IEEE J Quantum Electron 1984, **QE-20**:1507-11
3. Andersson PS, Kjellén E, Montán S, Svanberg K, Svanberg S, *Autofluorescence of various rodent tissues and human skin tumour samples*. Lasers Med Sci 1987, **2**:41-9
4. Kittrell C, Willett RL, de los Santos-Pacheo C, Ratliff NB, Kramer JR, Malk EG, Feld MS, *Diagnosis of fibrous arterial atherosclerosis using fluorescence*. Appl Opt 1985, **24**:2280-1
5. Deckelbaum LI, Lam JK, Cabin HS, Clubb KS, Long MB, *Discrimination of normal and atherosclerotic aorta by laser-induced fluorescence*. Lasers Surg Med 1987, **7**:330-5
6. Andersson PS, Gustafson A, Stenram U, Svanberg K, Svanberg S, *Diagnosis of arterial atherosclerosis using laser-induced fluorescence*. Lasers Med Sci 1987, **2**:261-6
7. Figge FHJ, Weiland GS, Manganiello LOJ, *Cancer detection and therapy. Affinity of neoplastic, embryonic, and traumatazied regenerating tissues for porphyrins and metalloporphyrins*. Proc Soc Exp Biol Med 1948, **68**:640-1
8. Lipson RL, Baldes EJ, Olsen AM, *The use of a derivative of haematoporphyrin in tumour detection*. J Nat Cancer Inst 1961, **26**:1-8
9. Profio AE, Doiron DR, Balchum OJ, Huth GC, *Fluorescence bronchoscopy for localization of carcinoma in situ*. Med Phys 1983, **10**:35-9
10. Kato H, Aizawa K, Ono J, Konaka C, Kawate N, Yoneyama K, Kinoshita K, Nishimiya K, Sakai H, Noguchi M, Tomono T, Kawasaki S, Tokuda Y, Hayata Y, *Clinical measurement of tumor fluorescence using a new diagnostic system with hematoporphyrin derivative, laser photoradiation and a spectroscope*. Lasers Surg Med 1984, **4**:49-58

11. Svanberg K, Kjellén E, Ankerst J, Montán S, Sjöholm E, Svanberg S, *Fluorescence studies of hematoporphyrin derivatives in normal and malignant rat tissue.* Cancer Res 1986, **46**:3803-8

12. See e.g. *Proceeding of the International Conference on Photodynamic Therapy*, Shopova M (ed), held in Sofia, Bulgaria, Oct 3-5, 1989

13. Profio AE, Balchum OJ, *Fluorescence diagnosis of cancer.* In; Kessel D (ed) *Methods in porphyrin photosensitization.* pp 43-50 Plenum, New York, 1985

14. Ankerst J, Montán S, Svanberg K, Svanberg S, *Laser-induced fluorescence studies of hematoporphyrin derivative (HPD) in normal and tumor tissue of rat.* Appl Spectr 1984, **38**:890-6

15. Profio AE, Doiron DR, Sarnaik J, *Fluorometer for endoscopic diagnosis of tumors.* Med Phys 1984, **11**:516-20

16. Hirano T, Ishizuka M, Suzuki K, Ishida K, Yasukawa M, Suzuki S, Miyaki S, Honma A, Suzuki M, Aizawa K, Kato H, Hayata Y, *Photodynamic cancer diagnosis and treatment system consisting of pulse lasers and an endoscopic spectro-image analyzer.* Lasers Life Sci 1989, **3**:1-18

17. Brodbeck KJ, Profio AE, Frewin T, Balchum OJ, *A system for real time fluorescence imaging in color for tumor diagnosis.* Med Phys 1987, **14**:637-9

18. Baumgartner R, Fisslinger H, Jocham D, Lenz H, Ruprecht L, Stepp H, Unsöld E, *A fluorescence imaging device for endoscopic detection of early stage cancer-instrumental and experimental studies.* Photochem Photobiol 1987, **46**:759-64

19. Montán S, Svanberg K, Svanberg S, *Multicolor imaging and contrast enhancement in cancer-tumor localization using laser-induced fluorescence in hematoporphyrin-derivative-bearing tissue.* Opt Lett 1985, **10**:56-8

20. Andersson PS, Montán S, Svanberg S, *Multispectral system for medical fluorescence imaging.* IEEE J Quantum Electron 1987, **QE-23**:1798-805

21. Andersson-Engels S, Gustafson A, Johansson J, Stenram U, Svanberg K, Svanberg S, *Laser-induced fluorescence in localizing atherosclerotic lesions.* Lasers Med Sci 1989, **4**:171-81

22. Andersson-Engels S, Brun A, Kjellén E, Salford LG, Strömblad L-G, Svanberg K, Svanberg S, *Identification of brain tumours in rats using laser-induced fluorescence and haematoporphyrin derivative.* Lasers Med Sci 1989, (in press)